Basic Research in Cardiology (2019) 114:42
https://doi.org/10.1007/s00395-019-0749-7

ORIGINAL CONTRIBUTION

Junctophilin-2 is a target of matrix metalloproteinase-2 in myocardial ischemia–reperfusion injury

Brandon Y. H. Chan[1] · Andrej Roczkowsky[1] · Woo Jung Cho[2] · Mathieu Poirier[1] · Tim Y. T. Lee[1] · Zabed Mahmud[3] · Richard Schulz[1]

Received: 18 April 2019 / Accepted: 2 September 2019

Abstract

Junctophilin-2 is a structural membrane protein that tethers T-tubules to the sarcoplasmic reticulum to allow for coordinated calcium-induced calcium release in cardiomyocytes. Defective excitation–contraction coupling in myocardial ischemia–reperfusion (IR) injury is associated with junctophilin-2 proteolysis. However, it remains unclear whether preventing junctophilin-2 proteolysis improves the recovery of cardiac contractile dysfunction in IR injury. Matrix metalloproteinase-2 (MMP-2) is a zinc and calcium-dependent protease that is activated by oxidative stress in myocardial IR injury and cleaves both intracellular and extracellular substrates. To determine whether junctophilin-2 is targeted by MMP-2, isolated rat hearts were perfused in working mode aerobically or subjected to IR injury with the selective MMP inhibitor ARP-100. IR injury impaired the recovery of cardiac contractile function which was associated with increased degradation of junctophilin-2 and damaged cardiac dyads. In IR hearts, ARP-100 improved the recovery of cardiac contractile function, attenuated junctophilin-2 proteolysis, and prevented ultrastructural damage to the dyad. MMP-2 was co-localized with junctophilin-2 in aerobic and IR hearts by immunoprecipitation and immunohistochemistry. In situ zymography showed that MMP activity was localized to the Z-disc and sarcomere in aerobic hearts and accumulated at sites where the striated JPH-2 staining was disrupted in IR hearts. In vitro proteolysis assays determined that junctophilin-2 is susceptible to proteolysis by MMP-2 and in silico analysis predicted multiple MMP-2 cleavage sites between the membrane occupation and recognition nexus repeats and within the divergent region of junctophilin-2. Degradation of junctophilin-2 by MMP-2 is an early consequence of myocardial IR injury which may initiate a cascade of sequelae leading to impaired contractile function.

Keywords Ischemia–reperfusion injury · Myocardial infarction · Matrix metalloproteinase · Junctophilin · Excitation–contraction coupling · Oxidative stress

Brandon Y. H. Chan and Andrej Roczkowsky contributed equally.

Electronic supplementary material The online version of this article (https://doi.org/10.1007/s00395-019-0749-7) contains supplementary material, which is available to authorized users.

✉ Richard Schulz
richard.schulz@ualberta.ca

Brandon Y. H. Chan
byc@ualberta.ca

Andrej Roczkowsky
roczkows@ualberta.ca

Woo Jung Cho
woojung.cho@ualberta.ca

Mathieu Poirier
poirier1@ualberta.ca

Tim Y. T. Lee
yitingti@ualberta.ca

Zabed Mahmud
zabed@ualberta.ca

[1] Departments of Pediatrics and Pharmacology, Mazankowski Alberta Heart Institute, 462 Heritage Medical Research Centre, University of Alberta, Edmonton, AB T6G 2S2, Canada

[2] Faculty of Medicine and Dentistry Cell Imaging Centre, University of Alberta, Edmonton, AB, Canada

[3] Department of Biochemistry, University of Alberta, Edmonton, AB, Canada

Published online: 10 September 2019

Introduction

Ischemic heart disease is one of the leading causes of global mortality and morbidity [17]. While timely restoration of blood flow to the heart critically limits the ischemic insult, reperfusion causes additional injury to the myocardium and coronary microvasculature [19]. Unfortunately, attempts to mitigate reperfusion injury have failed to translate in the clinical setting, largely due to the complex pathophysiology of myocardial ischemia–reperfusion (IR) injury [15, 16, 19]. IR injury disrupts excitation–contraction coupling and impairs myocardial contractility [24]. Increased oxidative stress [10], intracellular calcium overload [17], and damage to dyadic junctions [13] are amongst several important mechanisms which underlie defective excitation–contraction coupling and impaired cardiac contractile function in IR injury.

Excitation–contraction coupling is the critical process in which an action potential is converted into mechanical contraction of the heart [9]. Cardiomyocyte contraction is tightly controlled by calcium-induced calcium release, whereby extracellular calcium enters through voltage-gated calcium channels, which then activates calcium efflux from the sarcoplasmic reticulum through type 2 ryanodine receptors [4, 39]. Calcium-induced calcium release depends on the propinquity between T-tubules and the terminal cisternae of the sarcoplasmic reticulum network [18, 29]. The T-tubule-sarcoplasmic reticulum junction is anchored by a family of proteins known as junctophilin (JPH) [34]. Of the four known members of the JPH family [12], JPH-2 is the predominant isoform expressed in the heart and cardiomyocytes [34].

JPH-2 is a structural membrane protein which tethers T-tubules across a 12- to 15-nm junctional cleft to the sarcoplasmic reticulum to allow for coordinated calcium-induced calcium release in cardiomyocytes [11, 34]. JPH-2 consists of eight membrane occupation and recognition nexus (MORN) motifs in the amino-terminal region and a transmembrane domain in its C-terminus which anchors it to the plasma membrane and sarcoplasmic reticulum, respectively [34]. JPH-2 is localized near the Z-disc region of the sarcomere in close spatial proximity to type 2 ryanodine receptors [47]. Cardiac-specific knockdown of JPH-2 reduces the number of junctional membrane complexes, impairs cardiac contractility, and causes heart failure in mice [36]. Similarly, reduced levels of JPH-2 have been reported in heart failure and this was associated with ultrastructural uncoupling between the T-tubule and sarcoplasmic reticulum junction, resulting in cardiac contractile dysfunction [23, 27, 38, 41, 44, 46]. More recently, loss of JPH-2 was reported in acute myocardial IR injury through the proteolytic activity of calpains [13, 28]. However, it remains unclear whether preventing JPH-2 proteolysis ameliorates cardiac contractile dysfunction in IR injury.

Matrix metalloproteinase-2 (MMP-2) is a zinc- and calcium-dependent protease best known for its ability to remodel extracellular matrix proteins [3]. Beyond the extracellular matrix, MMP-2 is also localized in many subcellular locales within the cardiomyocyte including the sarcomere, nucleus, mitochondria, mitochondria-associated membrane, sarcoplasmic reticulum, and caveolae [20]. Within the sarcomere, MMP-2 is primarily localized to the Z-disc as well as the I- and A-band regions [1, 40]. During reperfusion, a burst of reactive oxygen and nitrogen species including peroxynitrite is generated in the ischemic myocardium [45]. Peroxynitrite directly activates MMP-2 [37], where it proteolyzes structural and contractile sarcomeric proteins such as α-actinin, myosin light chain-1, troponin I, and titin [1, 3, 31, 33, 40]. Inhibition of MMP-2 prevented the degradation of sarcomeric proteins and improved the recovery of cardiac contractile function during reperfusion [1, 20, 31, 40].

Given that MMP-2 and JPH-2 are enriched along the Z-disc region of the sarcomere in cardiomyocytes [1, 47], we determined whether JPH-2 is a target of MMP-2 in myocardial IR injury. In this study, MMP-2 contributes to JPH-2 proteolysis in IR injury, an effect that was prevented with an MMP inhibitor. Preventing JPH-2 proteolysis by MMP inhibition was associated with improved cardiac contractile function during IR. In silico analysis predicted multiple putative MMP-2 cleavage sites in the cytosolic domain of JPH-2 and in vitro proteolysis studies demonstrated that endogenous JPH-2 is susceptible to proteolysis by MMP-2.

Methods

All experiments involving animals in this study were approved by the University of Alberta Institutional Animal Care and Use Committee, in accordance to the Guide to the Care and Use of Experimental Animals published by the Canadian Council on Animal Care (CCAC).

Isolated working rat heart perfusion

Male Sprague–Dawley rats (300–400 g) from Charles River Laboratories (Saint-Constant, QC), were anesthetized with 240 mg kg^{-1} sodium pentobarbital (i.p.). Hearts were excised, rinsed in ice-cold Krebs–Henseleit solution (118 mM NaCl, 25 mM $NaHCO_3$, 4.7 mM KCl, 1.2 mM $MgSO_4$, 1.2 mM KH_2PO_4, 11 mM glucose, 0.5 mM EDTA, and 3 mM $CaCl_2$), and then cannulated at the aorta. Hearts were perfused in Langendorff mode for 10 min (pre-equilibration time) at constant pressure (60 mmHg) with oxygenated Krebs–Henseleit solution (95% O_2, 5% CO_2) at 37 °C. During this time, non-cardiac tissue was removed from the

heart and the left atrium was cannulated. Hearts were then perfused in working mode with recirculating Krebs–Henseleit solution (100 mL volume) with the addition of 100 µU insulin (Humulin R, Lilly, Indianapolis, IN, USA), 0.1% bovine serum albumin (Equitech-Bio Inc, Kerrville, TX, USA), and 5 mM sodium pyruvate. Hearts were maintained at 37 °C for the duration of the experiment using a water-jacketed glass heart chamber. Perfusate entered the left atria with a hydrostatic preload pressure of 15 mmHg and was then ejected from the left ventricle against a hydrostatic afterload pressure of 75 mmHg. Cardiac output and aortic flow were measured with in-line ultrasonic flow probes (Transonic Systems Inc, Ithaca, NY, USA). Heart rate and peak systolic pressure were measured using a pressure transducer (Harvard Apparatus, Holliston, MA, USA) in the aortic outflow line. Cardiac work, the product of cardiac output and peak systolic pressure, was used as an index of mechanical function. Hearts were equilibrated for 10 min in working mode before initiating the experiment ($t = 0$ min).

Following equilibration, control hearts were perfused aerobically for 70 min. IR hearts were perfused aerobically for 20 min and then subjected to 20 min global, no-flow ischemia, followed by 30 min aerobic perfusion. To test the effect of an MMP inhibitor, either 10 µM ARP-100 or its vehicle (0.05% v/v DMSO) were added into the recirculating perfusate 10 min into the timed perfusion. A schematic diagram of the perfusion protocol is illustrated in Fig. 1a.

Preparation of heart samples

For biochemical assays, the hearts were flash frozen at the end of the experiment ($t = 70$ min) using Wollenberger clamps. The frozen ventricles were pulverized using a mortar and pestle cooled by liquid nitrogen. Pulverized tissue was weighed and homogenized in 1:10 (w/v) radioimmunoprecipitation assay (RIPA) buffer (Sigma-Aldrich) containing 0.1% proteinase inhibitor cocktail using a PRO200 tissue homogenizer (Bio-Gen, Cambridge, MA, USA) for 2 min (in cycles of 15 s on, 15 s off) at 4 °C. The homogenate was then centrifuged at 10,000×*g* for 10 min at 4 °C. The supernatant (ventricular extract) was collected, aliquoted and stored at − 80 °C. Total protein concentration was measured by bicinchoninic acid assay using bovine serum albumin as a standard. A portion of the ventricular extract was used for gelatin zymography (see Supplementary Material for details).

An identical but separate series of heart perfusions were done as above in order to collect fresh heart tissue for microscopy experiments. For in situ zymography, a portion of the left ventricle of each heart was isolated and fixed overnight at 4 °C in zinc fixative (36.7 mM $ZnCl_2$, 27.3 mM zinc acetate dihydrate, 0.63 mM calcium acetate, and 0.1 M Tris, pH 7.6). Zinc-fixed left ventricular tissue was paraffin-embedded and then stored at 4 °C until use.

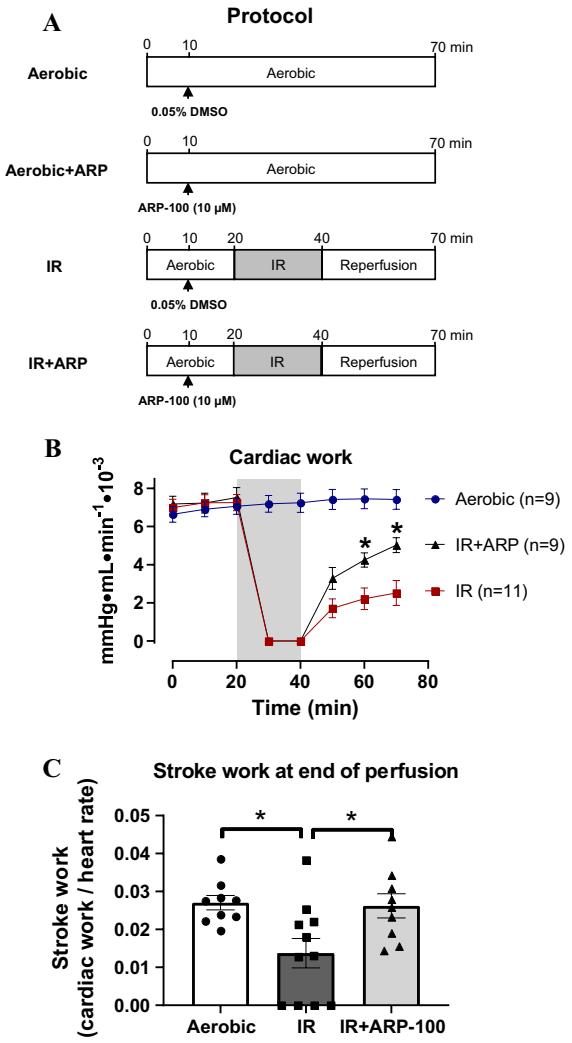

Fig. 1 **a** Schematic diagram of the working heart perfusion protocol in aerobic, aerobic + ARP, ischemic-reperfused (IR), and IR + ARP rat hearts. IR hearts were subject to 20 min global, no-flow ischemia, followed by 30 min of aerobic reperfusion. 10 µM ARP-100 or 0.05% DMSO (vehicle) was added to the recirculating buffer 10 min into perfusion. **b** Cardiac contractile performance was measured by cardiac work, the product of peak systolic pressure and cardiac output. ARP-100 significantly improved the recovery of cardiac work compared to IR hearts at the end of reperfusion. **c** Stroke work (cardiac work normalized to heart rate) was measured at the end of reperfusion. *$p < 0.05$ vs IR

For immunohistochemistry experiments, a portion of the left ventricle was fixed in 4% paraformaldehyde in 0.1 M Sorensen's phosphate buffered solution (Electron Microscopy Sciences, Hatfield, PA, USA) overnight at 4 °C and then cryopreserved in 30% sucrose in 0.1 M Sorenson's phosphate buffered solution overnight at 4 °C. Cryopreserved ventricular tissue was snap frozen in Tissue-Tek Optimal Cutting Temperature (OCT) compound (VWR, Radnor, PA, USA) cooled in liquid nitrogen and stored at − 80 °C until use.

For conventional transmission electron microscopy experiments, left ventricular sections were fixed in a mixture containing 3% glutaraldehyde and 3% paraformaldehyde in 0.1 M sodium cacodylate buffer at 4 °C.

Western blot analysis

Ventricular extract proteins (10 µg of total protein) were separated on 8% polyacrylamide gels by electrophoresis. Proteins were transferred onto polyvinylidene difluoride membranes (Bio-Rad, Hercules, CA, USA). Membranes were immunoblotted with primary monoclonal antibodies against JPH-2 (1:4000, #40-5300, Thermo Fisher Scientific, Waltham, MA, USA) and GAPDH (2118S, Cell Signaling Technology, Danvers, MA, USA). Primary antibodies were then probed with secondary goat anti-rabbit IgG antibodies (CLCC42007, Cedarlane, Burlington, ON, Canada). Protein bands were visualized using chemiluminescent detection reagent Clarity™ ECL western substrate (Bio-Rad) and exposed to autoradiography film.

MMP-2 binding to JPH-2 by co-immunoprecipitation

To determine whether MMP-2 interacts with JPH-2 in the heart, ventricular extracts (25 µg protein per sample) were diluted in RIPA buffer to a final volume of 200 µL and incubated with rabbit MMP-2 antibody (1:200, ab92536, Abcam, Cambridge, UK) or rabbit IgG isotype control (1:200, ab27472, Abcam) under rotatory agitation overnight at 4 °C. 50 µL of Protein G Sepharose bead slurry (ab193259, Abcam) was then added to each sample and incubated on a rotator for 4 h at 4 °C. The suspension was centrifuged (3000×*g*, 2 min, 4 °C) and the beads were washed with wash buffer (150 mM NaCl, 10 mM Tris, 1 mM EDTA, 1 mM EGTA, 0.2 mM sodium orthovanadate, and 1% Triton X-100, pH 7.4) three times at room temperature. The beads were resuspended in 2× Laemmli buffer, heat denatured at 95 °C for 5 min, and separated on 8% polyacrylamide gels for western blot analysis. After transfer, the PVDF membranes were probed with JPH-2 antibody (1:4000, #40-5300, Thermo Fisher Scientific) to determine whether MMP-2 is associated with JPH-2.

MMP-2 activity by in situ zymography

Paraffin-embedded, zinc-fixed left ventricular tissue was cut into 4 µm-thick sections and mounted onto Superfrost Plus glass slides (Fisher Scientific). Slides were deparaffinized in an ethanol series (100–70%) and then in water at room temperature. DQ gelatin is fluorescein-labeled gelatin substrate that is internally quenched unless it is cleaved by MMP-2 or MMP-9. Each ventricular section was incubated with 50 µg mL^{-1} DQ gelatin (Thermo Fisher Scientific) diluted in zymographic activity buffer (50 mM Tris–HCl, 150 mM NaCl, 5 mM $CaCl_2 \cdot 2H_2O$, and 0.05% NaN_3, pH 7.6) at 37 °C or 4 °C (autofluorescence control) for 4 h. Ventricular sections were also incubated with DQ gelatin substrate in the presence of MMP inhibitor EDTA (20 mM) at 37 °C to determine the contribution of MMP activity to detectable gelatinolytic activity, as previously described [14]. After incubation with DQ gelatin, nuclei were stained with 1 µg mL^{-1} DAPI (Sigma-Aldrich, St. Louis, MO, USA). Slides were washed with PBS before mounting with coverslips using Vectashield mounting medium (H-1400, Vector Laboratories, Burlingame, CA, USA).

Gelatinolytic activity was visualized with a Leica TCS SP5 confocal laser scanning microscope (Wetzlar, Germany) using a 488 nm argon ion laser with a band pass 508–558 nm filter. DAPI was visualized using a 405 nm diode laser with a bandpass 425–485 nm filter. Images were collected sequentially with a line average of 4 at a resolution of 1024 × 1024 pixels. Three fields of view were acquired from each left ventricle. Left ventricles from three rat hearts were analyzed for each group.

Transmission electron microscopy

For conventional transmission electron microscopy, prefixed left ventricular tissue was post-fixed in a mixture of 2% osmium tetroxide and 1.5% potassium ferrocyanide in 0.1 M sodium cacodylate buffer (Electron Microscopy Sciences). The tissue was then dehydrated in ethanol, embedded in Spurr's resin (Electron Microscopy Sciences), and thermally polymerized at 70 °C. The polymerized tissue was longitudinally trimmed along the myofilaments and cut using an ultramicrotome with a diamond knife (DiATOME, Hatfield, PA, USA). 70 nm ultrathin sections were obtained and transferred to a 200-mesh bare copper grid. Contrast was enhanced with staining with uranyl acetate and lead citrate (Electron Microscopy Sciences). The sections were observed with a Hitachi H-7650 transmission electron microscope (Toronto, ON, Canada) with an 11 megapixel EMCCD.

Colocalization of MMP-2 to JPH-2 by immunofluorescence

Left ventricular tissue embedded in OCT compound was cut into 4 µm-thick sections and mounted onto Superfrost Plus slides. Sections were quenched with PBS containing 0.4 M glycine for 15 min and then incubated with blocking buffer (Image-iT FX signal enhancer, Invitrogen, Carlsbad, CA, USA) for 1 h at room temperature. Double immunolabeling was performed by staining with mouse anti-MMP-2 (1:100, MAB3308, Millipore, Burlington, MA, USA) and rabbit anti-JPH-2 (1:100, #40-5300, Thermo Fisher Scientific), diluted in PBS containing 10% goat serum overnight

at 4 °C. Sections were then incubated with secondary antibodies conjugated to fluorescent dyes (Alexa Fluor 555 goat anti-mouse, 1:1000, A21127, Invitrogen; Alexa Fluor 488 goat anti-rabbit, 1:1000, A11008, Invitrogen) diluted in PBS containing 10% goat serum for 1 h at room temperature. The slides were mounted with coverslips using ProLong Diamond Antifade mountant (Invitrogen) and cured at room temperature for 24 h before imaging.

Immunolabelled ventricular sections were visualized with a Leica TCS SP5 laser scanning confocal microscope. Alexa Fluor 488 signal was captured using a 488 nm argon ion laser with a band pass 498–538 nm filter. Alexa Fluor 555 signal was captured using a 543 nm Green HeNe laser with a band pass 553–613 nm filter. Line profile analysis was performed using Image Pro plus software (Media Cybernetics Inc., Rockville, MD, USA).

In vitro proteolysis of JPH-2 by MMP-2

As purified JPH-2 is not commercially available, ventricular extracts (4 µg total protein) from an aerobic heart were incubated with increasing amounts of activated human recombinant MMP-2 (5–500 ng) in the presence or absence of 30 µM ARP-100 for 30 min at 37 °C. In vitro proteolysis of JPH-2 by MMP-2 was repeated using three aerobic hearts. The reaction products were then separated on a 10% polyacrylamide gel, transferred, and immunoblotted for JPH-2 as described above. JPH-2 degradation was determined by quantifying the density of the JPH-2 band and normalizing it to GAPDH.

In silico-predicted JPH-2 cleavage sites by MMP-2

In silico prediction of JPH-2 cleavage sites by MMP-2 was performed using the online cleavage prediction server CleavPredict [22]. This online tool is optimized for MMPs and predicts substrate cleavage sites for 11 MMPs including MMP-2 by using a position weight matrix algorithm. There is currently no 3D crystal structure of JPH-2 available in Protein Data Bank. Therefore, the rat JPH-2 FASTA sequence (UniProt ID-Q2PS20) was entered into the CleavPredict query sequence section and MMP-2 was selected as the protease. The datasets from CleavPredict resulted from a high-throughout proteomic technique and proteome identification of protease cleavage sites were used to determine the substrate specificity profile of MMP-2 [22].

Statistical analysis

Data are expressed as mean ± SEM of n independent experiments. Working heart, in vitro degradation, and western blot data were analyzed by one-way ANOVA followed by Dunnett's or Tukey's post hoc test using GraphPad Prism 8 (GraphPad Software, La Jolla, CA, USA). p values < 0.05 were considered significant.

Results

MMP inhibitor ARP-100 improves cardiac contractile function in IR injury

Figure 1a illustrates the isolated working rat heart protocol for aerobic, aerobic + ARP, IR, and IR + ARP groups. Aerobic hearts exhibited no loss of cardiac contractile function, measured by cardiac work, for the entire 70 min of perfusion (Fig. 1b). A summary of the cardiac performance parameters at the end of perfusion is detailed in Table 1. IR hearts exhibited impaired recovery of contractile function during reperfusion compared to aerobic hearts (Fig. 1b). The MMP inhibitor ARP-100 significantly improved the recovery of cardiac work (Fig. 1b), as well as stroke work (Fig. 1c), cardiac output, and aortic flow during reperfusion compared to IR hearts (Table 1).

ARP-100 inhibits myocardial MMP-2 activity in situ

Gelatin zymography was performed on the ventricular extracts to estimate the levels of MMP-2 and MMP-9 activity. While there was abundant 72 kDa MMP-2 activity

Table 1 Cardiac performance parameters at the end of perfusion for the four groups of isolated working rat hearts

End of perfusion (70 min)	Aerobic ($n=9$)	Aerobic + ARP ($n=5$)	IR ($n=11$)	IR + ARP ($n=9$)
Cardiac work (mmHg mL min^{-1} 10^{-3})	7.4 ± 0.5	6.1 ± 1.1	2.5 ± 0.7*	5.0 ± 0.4‡
Peak systolic pressure (mmHg)	118 ± 3	110 ± 4	83 ± 16	120 ± 4
Cardiac output (mL min^{-1})	68.8 ± 3.4	60.8 ± 9.1	23.5 ± 5.7*	46.1 ± 3.1‡
Aortic flow (mL min^{-1})	46.6 ± 2.6	39.2 ± 8.7	9.6 ± 3.1*	24.9 ± 3.3‡
Coronary flow (mL min^{-1})	22.2 ± 1.6	21.6 ± 1.5	13.8 ± 3.1	21.2 ± 1.9
Heart rate (bpm)	276 ± 7	258 ± 15	123 ± 31*	203 ± 16

*$p < 0.05$ vs aerobic, $^{\ddagger}p < 0.05$ vs IR by one-way ANOVA followed by Tukey's post hoc test

and lower levels of 64 kDa MMP-2 activity, there was no detectable MMP-9 activity in the ventricular extracts (Online Fig. 1). This suggests that the MMP gelatinolytic activity measured by gelatin zymography is mainly attributed to MMP-2. In situ zymography was performed on left ventricular sections from aerobic, IR, and IR + ARP hearts to visualize the distribution of myocardial MMP-2 activity. There was no detectable autofluorescence in the ventricular sections from each group (Online Fig. 2a–c). Aerobic, IR, and IR + ARP ventricular sections incubated with DQ gelatin in the presence of EDTA (pan-MMP inhibitor) exhibited no gelatinolytic activity confirming this activity is MMP-dependent (Online Fig. 2d–f). Brightfield images revealed that IR hearts exhibited myofibrillar disorganization compared to aerobic hearts (Fig. 2a, b). IR + ARP hearts showed myofibrillar organization similar to aerobic hearts (Fig. 2c). In situ zymography revealed abundant MMP activity within the cardiomyocytes of aerobic and IR hearts, which was abolished in IR + ARP hearts (Fig. 2d–f). In particular, MMP activity was localized to the Z-disc of the sarcomere in aerobic hearts (Fig. 2d, g), whereas this activity was redistributed as intracellular clusters in IR hearts (Fig. 2e, h) and abolished in IR + ARP hearts (Fig. 2f, i).

ARP-100 prevents ultrastructural remodeling of the cardiac dyad in IR injury

Transmission electron micrographs of longitudinal sections of the left ventricle revealed significant differences in the ultrastructure of the cardiac dyad between aerobic and IR hearts. T-tubules, which are situated at the Z-disc in normal myocardium (Fig. 3a), were depleted in IR hearts (Fig. 3b). Most notably, IR + ARP hearts did not exhibit T-tubule loss in the left ventricle (Fig. 3c). Increased magnification of the cardiac dyad revealed the close proximity between the T-tubule and the terminal cisternae of the sarcoplasmic reticulum in aerobic hearts (Fig. 3d). This association was disrupted in IR hearts (Fig. 3e) and maintained in IR + ARP hearts (Fig. 3f).

MMP-2 contributes to JPH-2 proteolysis in IR injury

To determine whether MMP-2 contributes to JPH-2 proteolysis in myocardial IR injury, JPH-2 levels in ventricular extracts from aerobic, IR, and IR + ARP hearts were assessed by immunoblot. JPH-2 levels were unchanged between the three groups (Fig. 4a). Increased exposure of the immunoblots revealed a lower molecular weight band (~ 63 kDa) representing a putative JPH-2 degradation product in the

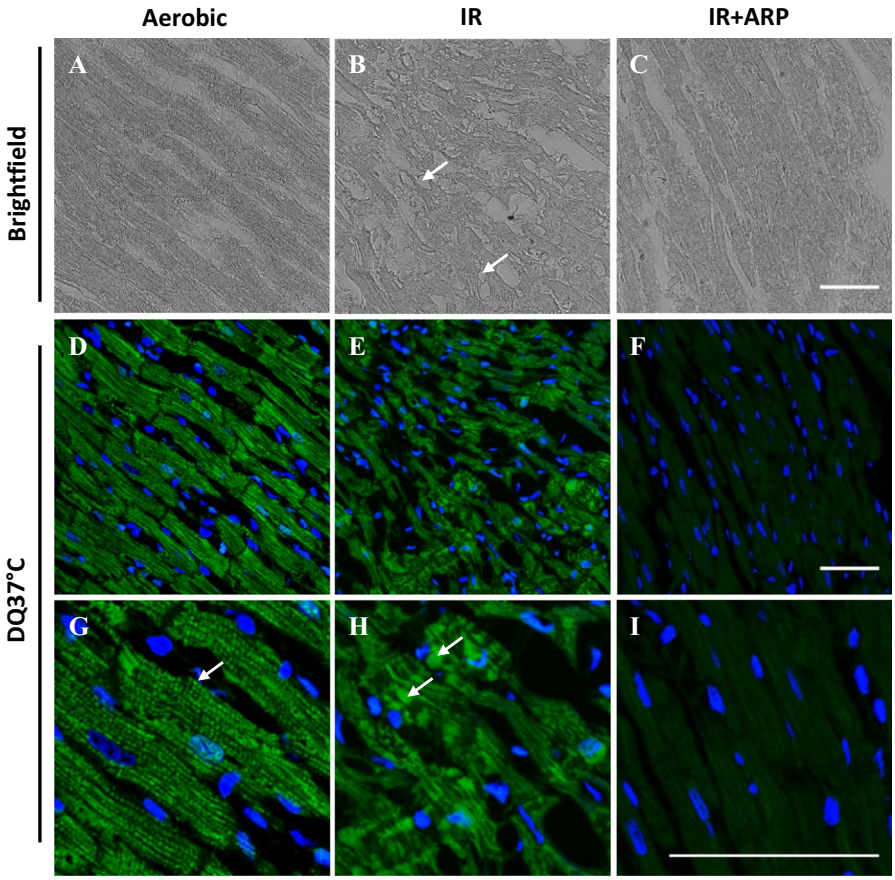

Fig. 2 IR injury redistributes intracellular MMP-2 activity in situ. **a–c** Brightfield images show that IR hearts exhibited abnormal myofibrillar morphology compared to aerobic and IR + ARP hearts. **d–f** In situ zymography detected MMP-2 activity within cardiomyocytes in aerobic and IR hearts, which was attenuated in IR + ARP hearts. **g–i** Higher magnification revealed that MMP-2 activity exhibited a striated pattern (arrows) in aerobic hearts, whereas MMP-2 activity appeared redistributed and clustered in IR hearts. Scale bar 50 µm. Representative of $n = 3$ hearts per group

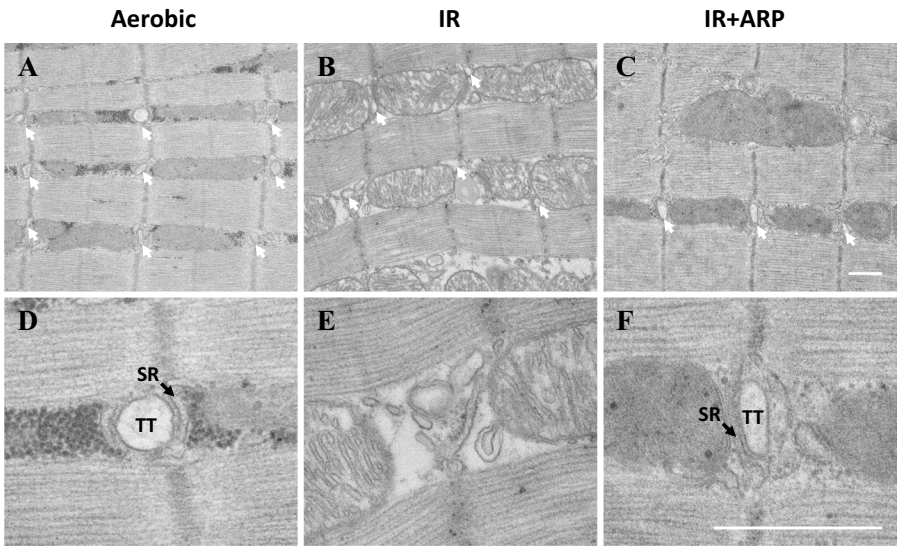

Fig. 3 ARP-100 prevents ultrastructural remodeling of the cardiac dyad in IR injury. **a–c** Conventional transmission electron microscopy showed the loss of T-tubules (white arrows) in IR hearts compared to aerobic and IR + ARP hearts. **d–f** The junction between T-tubules (TT) and the sarcoplasmic reticulum (SR, black arrow) was disrupted in IR hearts, which was prevented by ARP-100. Scale bar 500 nm. Images shown are representative of 25 images from $n = 3$ hearts per group

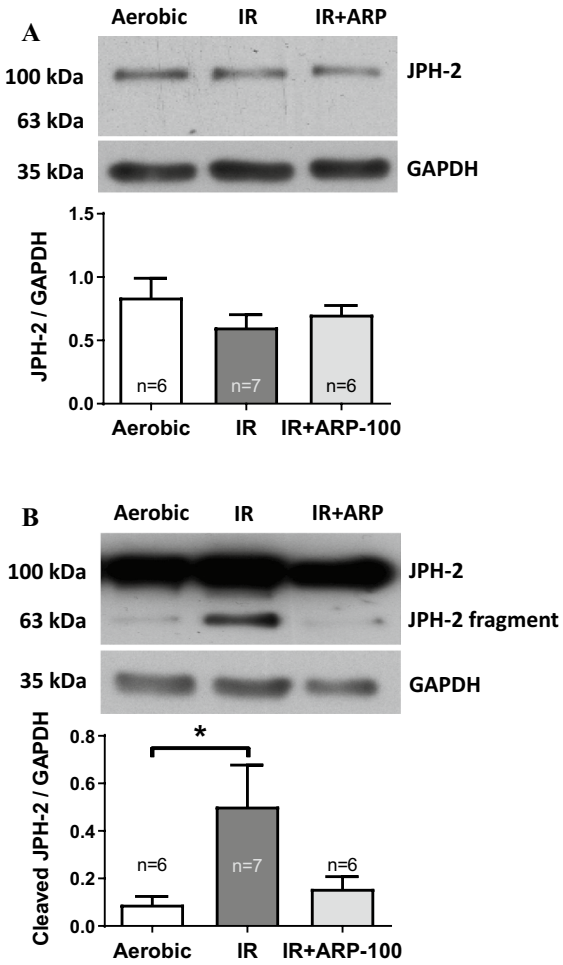

Fig. 4 Levels of JPH-2 and its degradation product in ventricular extracts from isolated rat hearts. **a** JPH-2 protein levels were unchanged between aerobic, IR, and IR + ARP hearts. **b** IR hearts exhibited a significant increase in a 63 kDa JPH-2 degradation product, an effect that was prevented by ARP-100. Bar graphs represent mean ± SEM. *$p < 0.05$

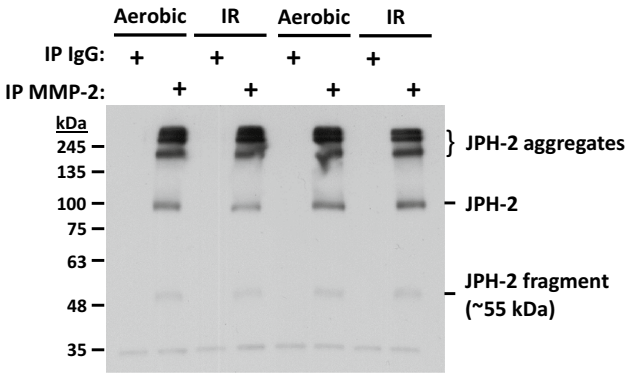

Fig. 5 MMP-2 is associated with JPH-2 in aerobic and IR hearts. A JPH-2 immunoblot of MMP-2 immunoprecipitates from aerobic and IR hearts revealed that MMP-2 is bound to JPH-2 aggregates, JPH-2 monomer, and a putative JPH-2 degradation product. Representative of four independent experiments

ventricular extracts from each group (Fig. 4b). More importantly, IR hearts exhibited a fivefold increase in JPH-2 degradation compared to aerobic hearts (Fig. 4b), which was attenuated in the IR + ARP hearts.

MMP-2 is co-localized to JPH-2 in the heart

In order to detect a possible interaction between MMP-2 and JPH-2 in the rat heart, MMP-2 was immunoprecipitated from ventricular extracts and then probed for JPH-2 by immunoblot. Full-length JPH-2, putative JPH-2 aggregates, and a putative lower molecular weight (~ 55 kDa) JPH-2 degradation product were detected in both aerobic and IR hearts (Fig. 5).

Given that MMP-2 and JPH-2 are both enriched in the Z-disc region of the sarcomere [1, 47], colocalization of MMP-2 and JPH-2 was assessed by immunofluorescence.

A control where the primary antibody was omitted and only the secondary antibody was used showed an absence of non-specific binding in the aerobic heart (Online Fig. 3a, b). JPH-2 staining in the left ventricle was consistent with sarcomeric Z-disc structures (Fig. 6a). In aerobic hearts, MMP-2 was primarily localized to Z-discs (Fig. 6b) and, to a lesser degree, between adjacent Z-discs as shown by the line profile analysis (Fig. 6d). The MMP-2 staining between the Z-discs is likely localized in the cytosol and/or the M-line region of the sarcomere [1]. When MMP-2 and JPH-2 signals were merged, MMP-2 was co-localized to JPH-2 in the heart (Fig. 6c, d). IR hearts exhibited disrupted JPH-2 staining as evidenced by the partial loss of JPH-2 striated staining pattern and an aggregate-like accumulation of JPH-2 (Fig. 6e), which was also seen for MMP-2 (Fig. 6f). MMP-2 was colocalized with JPH-2 in IR hearts, particularly in regions where the striated pattern of JPH-2 staining was disrupted (Fig. 6g).

Endogenous JPH-2 is susceptible to proteolysis by MMP-2

Using CleavPredict, we identified 30 potential cleavage sites in JPH-2 by MMP-2 along with their predicted secondary structure and corresponding mass of both N- and C-terminal cleavage fragments. We tabulated the ten cleavage sites with the highest position weight matrix score (Table 2). As expected, no cleavage sites were predicted within the highly structured regions of JPH-2, namely the α-helix and transmembrane domain to the sarcoplasmic reticulum (Fig. 7a, Table 2). Most of the cleavage sites were predicted in the N-terminal region of junctophilin between MORN repeats and within the C-terminal divergent region. We then aligned the predicted cleavage sites with the active site specificity profiling dataset of MMP-2 [8] to determine its similarity to the substrate amino acid specificity from P5–P5′. Our results show significant similarities with 57% sequence homology to the sequence specificity profile of MMP-2 from P3–P3′ position (Table 2).

In order to test the susceptibility of JPH-2 to proteolysis by MMP-2, ventricular extracts prepared from aerobic hearts were incubated at 37 °C with increasing amounts of MMP-2 for 30 min. A JPH-2 immunoblot revealed that 50 ng of MMP-2 degraded approximately 50% of endogenous JPH-2 (Fig. 7b, c). At 500 ng of MMP-2, JPH-2 was fully degraded in the ventricular extracts. MMP-2 dependent JPH-2 proteolysis was prevented by ARP-100 (Fig. 7b, c). This demonstrates that endogenous JPH-2 is susceptible to proteolysis by MMP-2 in a concentration-dependent manner.

Discussion

Elucidating the mechanism of JPH-2 proteolysis is essential to understanding impaired myocardial contractility in IR injury. In this study, we demonstrated that JPH-2, a key structural component of the cardiac dyad, is a target of MMP-2 in acute myocardial IR injury. In situ zymography analysis revealed that MMP-2 activity is localized to the Z-disc region of the sarcomere in aerobic rat hearts. IR hearts showed increased JPH-2 degradation, disrupted cardiac dyads, and increased MMP-2 protein and activity

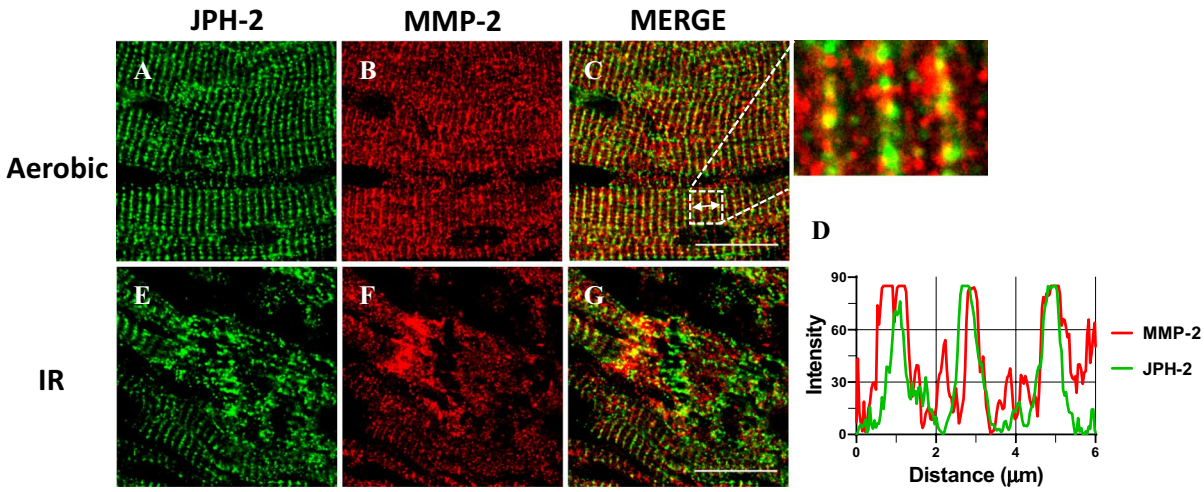

Fig. 6 MMP-2 co-localizes to JPH-2 in the heart. Left ventricular tissue sections from an aerobic heart stained for **a** JPH-2, **b** MMP-2, and **c** merged image (colocalization seen as yellow). **d** Profile analysis of the line indicated in the magnified inset shows colocalization of JPH-2 and MMP-2. IR hearts exhibited regions with disrupted **e** JPH-2 and **f** MMP-2 staining. **g** Merged image shows that colocalization particularly occurs where the striated pattern for JPH-2 was disrupted. Images are representative of sections from $n=4$ hearts. Scale bar 20 μm

Table 2 Top ten positional weight matrix (PWM) score for MMP-2 cleavage sites within the cytoplasmic region of rat JPH-2 according to CleavPredict

P1	Residues	PWM score	N-mass (kDa)	C-mass (kDa)	P3–P3′ (% homology) (%)
165	LSS-LRS	7.24	17.9	56.3	50
201	LSL-LAT	3.40	21.5	52.7	50
213	PGL-FTR	4.50	22.6	51.6	50
222	LGR-LRR	5.91	23.6	50.6	33
241	LSF-LKS	6.78	25.8	48.4	50
350	**VLP-LKS**	**5.07**	**37.6**	**36.6**	**67**
372	**AAA-IAR**	**3.79**	**40.0**	**34.3**	**83**
555	VAL-YRG	4.07	59.4	14.8	50
594	PSP-VSA	4.94	63.7	10.5	83
640	ARG-LSK	3.96	68.6	5.6	50
				Average	**57**

The predicted cleavage sites were aligned with the active site specificity profiling dataset of MMP-2 to determine the percent homology to MMP-2 cleavage motifs. Cleavage sites P1 350 and 372 (in bold) were predicted to produce degradation products with a similar molecular weight observed in IR hearts by gel electrophoresis

where normal striated JPH-2 staining was lost. In silico analysis predicted multiple MMP-2 cleavage sites between the MORN repeats and the divergent region of JPH-2. Endogenous JPH-2 in ventricular extracts was susceptible to proteolysis by MMP-2 in vitro. Inhibition of MMP-2 by ARP-100 attenuated JPH-2 proteolysis, prevented ultrastructural damage to the cardiac dyad, and improved the recovery of cardiac contractile function in IR injury. This indicates that JPH-2 proteolysis is an early consequence of MMP-2 activity during IR injury.

Although MMPs have been extensively studied for their roles in remodeling extracellular matrix proteins in long term (days to weeks) remodeling processes [32], MMPs also target non-matrix substrates [26] including intracellular proteins [20] in acute (seconds to minutes) pathophysiological processes. MMP-2 is maximally activated within minutes of ischemia–reperfusion [7]. Inhibition of MMP activity with o-phenanthroline, doxycycline, or ONO-4817 improved the recovery of cardiac contractile function in IR or peroxynitrite-induced injury by preventing the degradation of sarcomeric (troponin I, titin, and myosin light chain-1) [1, 31, 40] and cytoskeletal (α-actinin) [33] proteins. Consistent with previous reports, MMP inhibition with ARP-100, the most selective MMP-2 inhibitor available ($K_i = 12$ nM), improved cardiac work following IR injury. Although ARP-100 also inhibits MMP-3 ($K_i = 4500$ nM) and MMP-9 ($K_i = 200$ nM) [30, 35], MMP-2 is the MMP inhibited by ARP-100 in hearts as MMP-3 is not found in cardiomyocytes and MMP-9 activity was not detected in ventricular extracts.

JPH-2 is a structural membrane protein that plays an important role in the molecular organization of the juncture between the T-tubule and the sarcoplasmic reticulum in cardiac muscle cells [34]. JPH-2 allows coupling between L-type calcium channels and type 2 ryanodine receptors for calcium-induced calcium release [23, 36]. Alterations in JPH-2 expression have deleterious consequences on myocardial contractility by reducing the density of dyadic junctions and decreasing the efficiency of excitation–contraction coupling [23, 43, 46]. Furthermore, loss of JPH-2 is consistently found in several types of progressive heart failure including dilated, hypertrophic, and ischemic cardiomyopathies [23, 27, 46]. Recent studies have suggested the JPH-2 levels are reduced in acute myocardial IR injury [13, 28]. Loss of JPH-2 was prevented by the calpain inhibitor MDL-28170 [13], which also inhibits MMP-2 activity [2]. However, no JPH-2 degradation products were detected in the ventricular extracts without the addition of exogenous calcium or calpain [13, 28]. We found that IR injury caused JPH-2 degradation, marked by an increase in the levels of a 63 kDa JPH-2 fragment. JPH-2 degradation and IR-induced cardiac contractile dysfunction were attenuated by ARP-100. This indicates that preventing JPH-2 proteolysis with MMP inhibitors contributes to the recovery of cardiac contractile function.

Immunofluorescence and subcellular fractionation studies have localized MMP-2 in many subcellular locales, most prominently near the Z-disc region of the sarcomere in cardiomyocytes [1]. For the first time, we show that MMP-2 activity is localized to the Z-disc region in cardiomyocytes by in situ zymography in the isolated rat heart. Immunohistochemistry and in situ zymography showed that the localization of MMP-2 activity is consistent with the striated JPH-2 staining pattern observed in aerobic hearts. This observation was consistent with previous studies which reported the localization of MMP-2 to the Z-disc region of the sarcomere and the degradation of Z-disc proteins titin

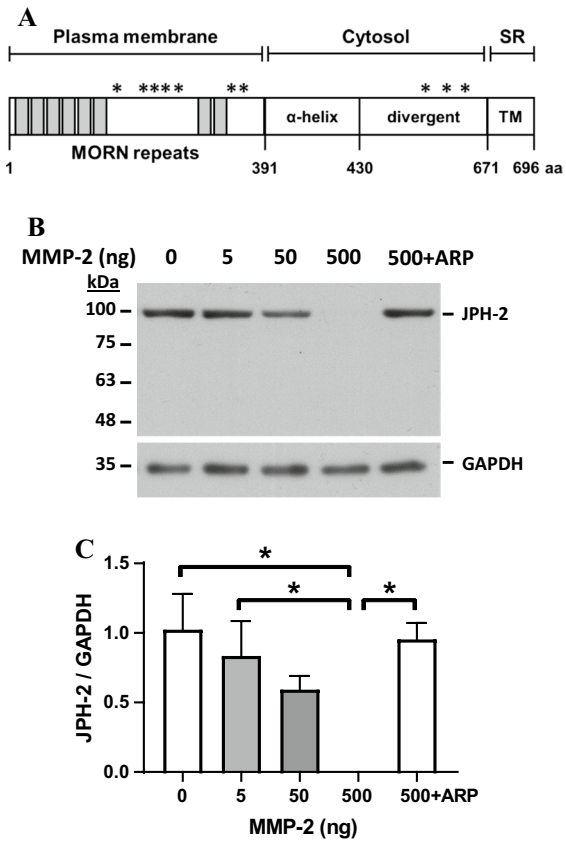

Fig. 7 JPH-2 is susceptible to proteolysis by MMP-2. **a** JPH-2 protein topology and the subcellular localization of its domains. MMP-2 cleavage sites in JPH-2 (*) were predicted between the MORN repeats and within the divergent region. **b** A JPH-2 immunoblot of ventricular extracts (20 µg protein) from an aerobic heart following incubation with MMP-2 (5–500 ng) for 30 min at 37 °C. MMP-2 cleaves JPH-2 in a concentration-dependent manner, which is prevented with 30 µM ARP-100 (ARP). Representative of three independent experiments. **c** Quantification of JPH-2 levels relative to GAPDH following proteolysis by MMP-2 ($n=3$). Bar graphs represent mean ± SEM. *$p<0.05$

[1] and α-actinin [33] in rat hearts subjected to oxidative stress injury. In contrast, intracellular MMP-2 protein and activity accumulated in the cytosol within the cardiomyocyte in regions where the striated pattern of JPH-2 staining was disrupted. It is likely that MMP-2 activity is initially enhanced at the Z-disc where it can target Z-disc proteins like JPH-2, α-actinin, and the N-terminal region of titin. Proteins in proximity to the Z-disc such as JPH-2 are likely most susceptible to proteolysis by MMP-2 activated during reperfusion. IR + ARP hearts showed little to no MMP-2 activity and exhibited normal myofibrillar morphology. These results suggest that the Z-disc region of the sarcomere is an important site and target of MMP-2 activity in myocardial IR injury.

Our results revealed that ARP-100 prevented the loss of T-tubules and disruption in the juncture between the T-tubule and the sarcoplasmic reticulum caused by IR injury. This highlights that JPH-2 proteolysis is MMP-2 dependent and is associated with ultrastructural remodeling of the cardiac dyad in IR injury. Loss of T-tubules following myocardial infarction has been linked to dyssynchronous calcium release from the sarcoplasmic reticulum [25]. JPH-2 degradation is an important determinant of T-tubule remodeling [42]. Cardiac-specific knockdown of JPH-2 has been shown to increase the intra-dyad junctional gap distance and impair excitation–contraction coupling in mice [36]. Guo et al. [13] showed that cardiomyocytes expressing truncated JPH-2 exhibit depressed calcium transients, signifying that expression of full-length JPH-2 is required to proper calcium handling and myocardial contractility. Our results suggest that MMP-2 mediated JPH-2 proteolysis is an important determinant of T-tubule remodeling and cardiac contractile dysfunction in IR injury. Cleavage of JPH-2 by MMP-2 may disrupt intracellular calcium homeostasis in IR injury. Protecting the structural integrity of JPH-2 in the heart may be an important determinant of whether an ischemic insult is reversible or irreversible.

We then tested the susceptibility of JPH-2 to proteolysis by MMP-2 by incubating the ventricular extracts from aerobic hearts to increasing concentrations of MMP-2. Endogenous JPH-2 was proteolyzed by MMP-2 in a concentration-dependent manner. Cleavage prediction software identified multiple putative MMP-2 cleavage sites in JPH-2. Due to the differences in the theoretical and the apparent molecular weight in gel electrophoresis, we predicted the JPH-2 cleavage sites that would correspond to a 63 kDa degradation product by estimating its apparent molecular weights from the calculated molecular weights of the N-terminal and C-terminal products. Two cleavage sites, P1 at 350 and 372, resulted in degradation products with an apparent molecular weight of around 63 kDa (Table 2). These cleavage sites are localized between the MORN repeats. JPH-2 has eight MORN repeats in the N-terminal region which interact with phospholipids, particularly sphingomyelin and phosphatidylcholine in the plasma membrane [34]. Cleavage of the MORN motifs in JPH-2 would disrupt the dyadic junction between the plasma membrane and the sarcoplasmic reticulum. Most notably, no cleavage sites were predicted in the cytosolic α-helix domain and the sarcoplasmic reticulum transmembrane domain, both of which are highly structured regions that are likely inaccessible for proteolytic degradation.

This study does not rule out that ARP-100 prevents MMP-2 from degrading other substrates of MMP-2 including troponin I, titin, myosin light chain 1, and α-actinin in IR injury. Myosin light chain 1 and troponin I may be targeted by MMP-2 later during reperfusion where MMP-2 activity accumulates in the bulk cytosol as shown by in situ zymography. Nor do we fully understand the potential contribution

of MMP-2 from other cardiac cells including the vascular endothelium and smooth muscle in IR injury [5, 21]. Our model of stunning injury using spontaneously beating hearts includes variances in heart rate and a proportion of hearts which show no functional recovery after reperfusion. Our study should be followed up by ex vivo studies using paced hearts and in models of in vivo stunning injury. It remains an open question whether MMP-2 pre-digests intracellular substrates for protein turnover via the ubiquitin–proteasome pathway under physiological conditions. Blocking excess MMP-2 activity during early reperfusion would prevent the proteolysis of intracellular proteins that are critical for myocardial function. Additionally, inhibiting excess MMP activity early upon reperfusion may also prevent ventricular remodeling as which occurs after myocardial infarction [6].

This study adds to the growing repertoire of intracellular MMP-2 substrates and increases our understanding of the role of MMP-2 in ischemic heart disease. These data provide compelling evidence that MMP-2 contributes to JPH-2 proteolysis in the pathogenesis of myocardial IR injury. Given that importance of JPH-2 in calcium-induced calcium release and cardiac excitation–contraction coupling, inhibiting its proteolysis by MMP-2 may be protective in ischemic heart disease.

Acknowledgements This work was supported by grants to R.S. from the Canadian Institutes of Health Research (Foundation #143299) and the Heart and Stroke Foundation of Canada. B.Y.C. was awarded a graduate studentship from the Women and Children's Health Research Institute, through the generous support of the Stollery Children's Hospital Foundation and the Royal Alexandra Hospital Foundation. A.R. was awarded graduate studentships from the Faculty of Medicine and Dentistry at the University of Alberta. Some experiments were performed at the University of Alberta Faculty of Medicine & Dentistry Cell Imaging Centre, which receives financial support from the Faculty of Medicine & Dentistry, the Department of Medical Microbiology & Immunology and Canada Foundation for Innovation awards to contributing investigators.

Compliance with ethical standards

Conflict of interest The authors have no conflict of interest.

References

1. Ali MA, Cho WJ, Hudson B, Kassiri Z, Granzier H, Schulz R (2010) Titin is a target of matrix metalloproteinase-2: implications in myocardial ischemia/reperfusion injury. Circulation 122:2039–2047. https://doi.org/10.1161/CIRCULATIONAHA.109.930222
2. Ali MA, Stepanko A, Fan X, Holt A, Schulz R (2012) Calpain inhibitors exhibit matrix metalloproteinase-2 inhibitory activity. Biochem Biophys Res Commun 423:1–5. https://doi.org/10.1016/j.bbrc.2012.05.005
3. Ali MAM, Fan F, Schulz R (2011) Cardiac sarcomeric proteins: novel intracellular targets of matrix metalloproteinase-2 in heart disease. Trends Cardiovasc Med 21:112–118
4. Bers DM (2002) Cardiac excitation–contraction coupling. Nature 415:198–205. https://doi.org/10.1038/415198a
5. Castro MM, Cena J, Cho WJ, Walsh MP, Schulz R (2012) Matrix metalloproteinase-2 proteolysis of calponin-1 contributes to vascular hypocontractility in endotoxemic rats. Arterioscler Thromb Vasc Biol 32:662–668. https://doi.org/10.1161/ATVBAHA.111.242685
6. Cerisano G, Buonamici P, Valenti R, Sciagrà R, Raspanti S, Santini A, Carrabba N, Dovellini EV, Romito R, Pupi A, Colonna P, Antoniucci D (2014) Early short-term doxycycline therapy in patients with acute myocardial infarction and left ventricular dysfunction to prevent the ominous progression to adverse remodelling: the TIPTOP trial. Eur Heart J 35:184–191. https://doi.org/10.1093/eurheartj/eht420
7. Cheung PY, Sawicki G, Wozniak M, Wang W, Radomski MW, Schulz R (2000) Matrix metalloproteinase-2 contributes to ischemia–reperfusion injury in the heart. Circulation 101:1833–1839
8. Eckhard U, Huesgen PF, Schilling O, Bellac CL, Butler GS, Cox JH, Dufour A, Goebeler V, Kappelhoff R, Keller UAD, Klein T, Lange PF, Marino G, Morrison CJ, Prudova A, Rodriguez D, Starr AE, Wang Y, Overall CM (2016) Active site specificity profiling of the matrix metalloproteinase family: proteomic identification of 4300 cleavage sites by nine MMPs explored with structural and synthetic peptide cleavage analyses. Matrix Biol 49:37–60. https://doi.org/10.1016/j.matbio.2015.09.003
9. Eisner DA, Caldwell JL, Kistamas K, Trafford AW (2017) Calcium and excitation–contraction coupling in the heart. Circ Res 121:181–195. https://doi.org/10.1161/CIRCRESAHA.117.310230
10. Ferdinandy P, Schulz R (2003) Nitric oxide, superoxide, and peroxynitrite in myocardial ischaemia–reperfusion injury and preconditioning. Br J Pharmacol 138:532–543. https://doi.org/10.1038/sj.bjp.0705080
11. Franzini-Armstrong C, Protasi F (1997) Ryanodine receptors of striated muscles: a complex channel capable of multiple interactions. Physiol Rev 77:699–729. https://doi.org/10.1152/physrev.1997.77.3.699
12. Garbino A, van Oort RJ, Dixit SS, Landstrom AP, Ackerman MJ, Wehrens XH (2009) Molecular evolution of the junctophilin gene family. Physiol Genom 37:175–186. https://doi.org/10.1152/physiolgenomics.00017.2009
13. Guo A, Hall D, Zhang C, Peng T, Miller JD, Kutschke W, Grueter CE, Johnson FL, Lin RZ, Song LS (2015) Molecular determinants of calpain-dependent cleavage of junctophilin-2 protein in cardiomyocytes. J Biol Chem 290:17946–17955. https://doi.org/10.1074/jbc.M115.652396
14. Hadler-Olsen E, Solli AI, Hafstad A, Winberg JO, Uhlin-Hansen L (2015) Intracellular MMP-2 activity in skeletal muscle is associated with type II fibers. J Cell Physiol 230:160–169. https://doi.org/10.1002/jcp.24694
15. Hausenloy DJ, Botker HE, Engstrom T, Erlinge D, Heusch G, Ibanez B, Kloner RA, Ovize M, Yellon DM, Garcia-Dorado D (2017) Targeting reperfusion injury in patients with ST-segment elevation myocardial infarction: trials and tribulations. Eur Heart J 38:935–941. https://doi.org/10.1093/eurheartj/ehw145
16. Hausenloy DJ, Garcia-Dorado D, Botker HE, Davidson SM, Downey J, Engel FB, Jennings R, Lecour S, Leor J, Madonna R, Ovize M, Perrino C, Prunier F, Schulz R, Sluijter JPG, Van Laake LW, Vinten-Johansen J, Yellon DM, Ytrehus K, Heusch G, Ferdinandy P (2017) Novel targets and future strategies for acute cardioprotection: position paper of the European Society of Cardiology Working Group on Cellular Biology of the Heart. Cardiovasc Res 113:564–585. https://doi.org/10.1093/cvr/cvx049

17. Hausenloy DJ, Yellon DM (2013) Myocardial ischemia-reperfusion injury: a neglected therapeutic target. J Clin Invest 123:92–100. https://doi.org/10.1172/JCI62874
18. Hayashi T, Martone ME, Yu Z, Thor A, Doi M, Holst MJ, Ellisman MH, Hoshijima M (2009) Three-dimensional electron microscopy reveals new details of membrane systems for Ca^{2+} signaling in the heart. J Cell Sci 122:1005–1013. https://doi.org/10.1242/jcs.028175
19. Heusch G, Gersh BJ (2017) The pathophysiology of acute myocardial infarction and strategies of protection beyond reperfusion: a continual challenge. Eur Heart J 38:774–784. https://doi.org/10.1093/eurheartj/ehw224
20. Hughes BG, Schulz R (2014) Targeting MMP-2 to treat ischemic heart injury. Basic Res Cardiol 109:424. https://doi.org/10.1007/s00395-014-0424-y
21. Kopaliani I, Martin M, Zatschler B, Bortlik K, Muller B, Deussen A (2014) Cell-specific and endothelium-dependent regulations of matrix metalloproteinase-2 in rat aorta. Basic Res Cardiol 109:419. https://doi.org/10.1007/s00395-014-0419-8
22. Kumar S, Ratnikov BI, Kazanov MD, Smith JW, Cieplak P (2015) CleavPredict: a platform for reasoning about matrix metalloproteinases proteolytic events. PLoS One 10:e0127877. https://doi.org/10.1371/journal.pone.0127877
23. Landstrom AP, Kellen CA, Dixit SS, van Oort RJ, Garbino A, Weisleder N, Ma J, Wehrens XH, Ackerman MJ (2011) Junctophilin-2 expression silencing causes cardiocyte hypertrophy and abnormal intracellular calcium-handling. Circ Heart Fail 4:214–223. https://doi.org/10.1161/CIRCHEARTFAILURE.110.958694
24. Louch WE, Ferrier GR, Howlett SE (2002) Changes in excitation–contraction coupling in an isolated ventricular myocyte model of cardiac stunning. Am J Physiol Heart Circ Physiol 283:H800–H810. https://doi.org/10.1152/ajpheart.00020.2002
25. Louch WE, Mork HK, Sexton J, Stromme TA, Laake P, Sjaastad I, Sejersted OM (2006) T-tubule disorganization and reduced synchrony of Ca^{2+} release in murine cardiomyocytes following myocardial infarction. J Physiol 574:519–533. https://doi.org/10.1113/jphysiol.2006.107227
26. McCawley LJ, Matrisian LM (2001) Matrix metalloproteinases: they're not just for matrix anymore! Curr Opin Cell Biol 13:534–540
27. Minamisawa S, Oshikawa J, Takeshima H, Hoshijima M, Wang Y, Chien KR, Ishikawa Y, Matsuoka R (2004) Junctophilin type 2 is associated with caveolin-3 and is down-regulated in the hypertrophic and dilated cardiomyopathies. Biochem Biophys Res Commun 325:852–856. https://doi.org/10.1016/j.bbrc.2004.10.107
28. Murphy RM, Dutka TL, Horvath D, Bell JR, Delbridge LM, Lamb GD (2013) Ca^{2+}-dependent proteolysis of junctophilin-1 and junctophilin-2 in skeletal and cardiac muscle. J Physiol 591:719–729. https://doi.org/10.1113/jphysiol.2012.243279
29. Pinali C, Bennett H, Davenport JB, Trafford AW, Kitmitto A (2013) Three-dimensional reconstruction of cardiac sarcoplasmic reticulum reveals a continuous network linking transverse-tubules: this organization is perturbed in heart failure. Circ Res 113:1219–1230. https://doi.org/10.1161/CIRCRESAHA.113.301348
30. Rossello A, Nuti E, Orlandini E, Carelli P, Rapposelli S, Macchia M, Minutolo F, Carbonaro L, Albini A, Benelli R, Cercignani G, Murphy G, Balsamo A (2004) New *N*-arylsulfonyl-*N*-alkoxyaminoacetohydroxamic acids as selective inhibitors of gelatinase A (MMP-2). Bioorgan Med Chem 12:2441–2450. https://doi.org/10.1016/j.bmc.2004.01.047
31. Sawicki G, Leon H, Sawicka J, Sariahmetoglu M, Schulze CJ, Scott PG, Szczesna-Cordary D, Schulz R (2005) Degradation of myosin light chain in isolated rat hearts subjected to ischemia–reperfusion injury: a new intracellular target for matrix metalloproteinase-2. Circulation 112:544–552. https://doi.org/10.1161/CIRCULATIONAHA.104.531616
32. Spinale FG (2007) Myocardial matrix remodeling and the matrix metalloproteinases: influence on cardiac form and function. Physiol Rev 87:1285–1342. https://doi.org/10.1152/physrev.00012.2007
33. Sung MM, Schulz CG, Wang W, Sawicki G, Bautista-Lopez NL, Schulz R (2007) Matrix metalloproteinase-2 degrades the cytoskeletal protein alpha-actinin in peroxynitrite mediated myocardial injury. J Mol Cell Cardiol 43:429–436. https://doi.org/10.1016/j.yjmcc.2007.07.055
34. Takeshima H, Komazaki S, Nishi M, Iino M, Kangawa K (2000) Junctophilins: a novel family of junctional membrane complex proteins. Mol Cell 6:11–22
35. Tuccinardi T, Martinelli A, Nuti E, Carelli P, Balzano F, Uccello-Barretta G, Murphy G, Rossello A (2006) Amber force field implementation, molecular modelling study, synthesis and MMP-1/MMP-2 inhibition profile of (*R*)- and (*S*)-*N*-hydroxy-2-(*N*-isopropoxybiphenyl-4-ylsulfonamido)-3-methylbutanamides. Bioorgan Med Chem 14:4260–4276. https://doi.org/10.1016/j.bmc.2006.01.056
36. van Oort RJ, Garbino A, Wang W, Dixit SS, Landstrom AP, Gaur N, De Almeida AC, Skapura DG, Rudy Y, Burns AR, Ackerman MJ, Wehrens XH (2011) Disrupted junctional membrane complexes and hyperactive ryanodine receptors after acute junctophilin knockdown in mice. Circulation 123:979–988. https://doi.org/10.1161/CIRCULATIONAHA.110.006437
37. Viappiani S, Nicolescu AC, Holt A, Sawicki G, Crawford BD, Leon H, van Mulligen T, Schulz R (2009) Activation and modulation of 72 kDa matrix metalloproteinase-2 by peroxynitrite and glutathione. Biochem Pharmacol 77:826–834. https://doi.org/10.1016/j.bcp.2008.11.004
38. Wagner E, Lauterbach MA, Kohl T, Westphal V, Williams GS, Steinbrecher JH, Streich JH, Korff B, Tuan HT, Hagen B, Luther S, Hasenfuss G, Parlitz U, Jafri MS, Hell SW, Lederer WJ, Lehnart SE (2012) Stimulated emission depletion live-cell super-resolution imaging shows proliferative remodeling of T-tubule membrane structures after myocardial infarction. Circ Res 111:402–414. https://doi.org/10.1161/CIRCRESAHA.112.274530
39. Wang SQ, Song LS, Lakatta EG, Cheng H (2001) Ca^{2+} signalling between single L-type Ca^{2+} channels and ryanodine receptors in heart cells. Nature 410:592–596. https://doi.org/10.1038/35069083
40. Wang W, Schulze CJ, Suarez-Pinzon W, Dyck J, Sawicki S, Schulz R (2002) Intracellular action of matrix metalloproteinase-2 accounts for acute myocardial ischemia and reperfusion injury. Circulation 106:1543–1549. https://doi.org/10.1161/01.cir.0000028818.33488.7b
41. Woo JS, Hwang JH, Ko JK, Weisleder N, Kim DH, Ma J, Lee EH (2010) S165F mutation of junctophilin 2 affects Ca^{2+} signalling in skeletal muscle. Biochem J 427:125–134. https://doi.org/10.1042/BJ20091225
42. Wu CY, Chen B, Jiang YP, Jia Z, Martin DW, Liu S, Entcheva E, Song LS, Lin RZ (2014) Calpain-dependent cleavage of junctophilin-2 and T-tubule remodeling in a mouse model of reversible heart failure. J Am Heart Assoc 3:e000527. https://doi.org/10.1161/JAHA.113.000527
43. Wu HD, Xu M, Li RC, Guo L, Lai YS, Xu SM, Li SF, Lu QL, Li LL, Zhang HB, Zhang YY, Zhang CM, Wang SQ (2012) Ultrastructural remodelling of Ca^{2+} signalling apparatus in failing heart cells. Cardiovasc Res 95:430–438. https://doi.org/10.1093/cvr/cvs195
44. Xu M, Zhou P, Xu SM, Liu Y, Feng X, Bai SH, Bai Y, Hao XM, Han Q, Zhang Y, Wang SQ (2007) Intermolecular failure of L-type Ca^{2+} channel and ryanodine receptor signaling

in hypertrophy. PLoS Biol 5:e21. https://doi.org/10.1371/journal.pbio.0050021
45. Yasmin W, Strynadka KD, Schulz R (1997) Generation of peroxynitrite contributes to ischemia–reperfusion injury in isolated rat hearts. Cardiovasc Res 33:422–432
46. Zhang HB, Li RC, Xu M, Xu SM, Lai YS, Wu HD, Xie XJ, Gao W, Ye H, Zhang YY, Meng X, Wang SQ (2013) Ultrastructural uncoupling between T-tubules and sarcoplasmic reticulum in human heart failure. Cardiovasc Res 98:269–276. https://doi.org/10.1093/cvr/cvt030
47. Ziman AP, Gomez-Viquez NL, Bloch RJ, Lederer WJ (2010) Excitation–contraction coupling changes during postnatal cardiac development. J Mol Cell Cardiol 48:379–386. https://doi.org/10.1016/j.yjmcc.2009.09.016